Electron Microscopy Imaging of Zinc Soaps Nucleation in Oil Paint

Hermans, J.; Osmond, G.; van Loon, A.; Iedema, P.; Chapman, R.; Drennan, J.; Jack, K.; Rasch, R.; Morgan, G.; Zhang, Z.; Monteiro, M.; Keune, K.

DOI
10.1017/s1431927618000387

Publication date
2018

Document Version
Final published version

Published in
Microscopy and Microanalysis

Microscopy and Microanalysis (2018), **24**, 318–322
doi:10.1017/S1431927618000387

Microscopy AND Microanalysis

Micrographia

Electron Microscopy Imaging of Zinc Soaps Nucleation in Oil Paint

Joen Hermans[1], Gillian Osmond[2], Annelies van Loon[1], Piet Iedema[1], Robyn Chapman[3], John Drennan[3], Kevin Jack[3], Ronald Rasch[3], Garry Morgan[4], Zhi Zhang[3], Michael Monteiro[5] and Katrien Keune[6]

[1]Van't Hoff Institute for Molecular Sciences, University of Amsterdam, 1098 XH Amsterdam, The Netherlands, [2]Queensland Art Gallery, Gallery of Modern Art of Modern Art, Brisbane, QLD 4101, Australia, [3]Centre for Microscopy and Microanalysis, University of Queensland, Brisbane, QLD 4072, Australia, [4]Department of MCD Biology, University of Colorado, Boulder, CO 80309, USA, [5]Australian Institute for Bioengineering and Nanotechnology, University of Queensland, Brisbane, QLD 4072, Australia and [6]Conservation and Restoration Department, Rijksmuseum, Museumstraat 1, 1071 XX Amsterdam, The Netherlands

Abstract

Using the recently developed techniques of electron tomography, we have explored the first stages of disfiguring formation of zinc soaps in modern oil paintings. The formation of complexes of zinc ions with fatty acids in paint layers is a major threat to the stability and appearance of many late 19th and early 20th century oil paintings. Moreover, the occurrence of zinc soaps in oil paintings leading to defects is disturbingly common, but the chemical reactions and migration mechanisms leading to large zinc soap aggregates or zones remain poorly understood. State-of-the-art scanning (SEM) and transmission (TEM) electron microscopy techniques, primarily developed for biological specimens, have enabled us to visualize the earliest stages of crystalline zinc soap growth in a reconstructed zinc white (ZnO) oil paint sample. *In situ* sectioning techniques and sequential imaging within the SEM allowed three-dimensional tomographic reconstruction of sample morphology. Improvements in the detection and discrimination of backscattered electrons enabled us to identify local precipitation processes with small atomic number contrast. The SEM images were correlated to low-dose and high-sensitivity TEM images, with high-resolution tomography providing unprecedented insight into the structure of nucleating zinc soaps at the molecular level. The correlative approach applied here to study phase separation, and crystallization processes specific to a problem in art conservation creates possibilities for visualization of phase formation in a wide range of soft materials.

Key words: electron microscopy, electron tomography, *in situ* microtome, zinc soaps

(Received 6 February 2017; revised 10 February 2018; accepted 17 April 2018)

Introduction

Incidences of zinc soap formation in oil paintings are being reported in escalating numbers (van der Weerd et al. 2003; Osmond et al., 2005; Rogola et al., 2010; Kaszowska et al., 2013; Helwig et al., 2014; Keune & Boeve-Jones, 2014), since being first characterized in destructive protrusions affecting Van Gogh's "Les Alyscamps" (van der Weerd et al., 2003). Shown to be a consequence of reactions between zinc white pigment and the drying oil binder, typically linseed, poppy seed or safflower oil, the responsible soaps were characterized as zinc carboxylates of predominantly stearic and palmitic acid. The same fatty acids are associated with lead soaps found in some paintings produced using lead white, red lead or lead tin yellow (Noble et al., 2002; Higgett et al., 2003; Plater et al., 2003; Keune & Boon, 2007; Townsend et al., 2007; Centeno & Mahon, 2009; Chen-Wiegart et al., 2017). More reactive than lead white, zinc oxide offered a less toxic alternative to lead white and came to be widely used in modern paint formulations (Harley, 1970; Kuhn, 1986; Osmond, 2012). Zinc soaps display a strong tendency to accumulate within paint layers or at interfaces, contributing to disfigurement and structural instability of important artworks. The phenomenon is a major concern for art conservation. At this stage, there is no known remedial process, so improved understanding of the processes involved is urgently required.

Figure 1 shows a surface detail from an oil-based painting by Sir Frederic Leighton (1830–1896); soap formation has imparted a granular texture to the painting surface, changing it utterly from the porcelain smooth finish intended by the artist (Osmond et al., 2013). Microscopy of a small embedded paint sample showing the layer structure of the painting reveals a large accumulation of predominantly zinc palmitate and zinc stearate within a lower layer. The growth of the soap mass has deformed the paint layers above, and lumps are visible to the naked eye. In other instances, growths may erupt and blister through the image surface, demonstrating the destructive forces involved and the potential risk zinc soaps pose for the long-term stability of oil paintings. Other changes associated with zinc soap formation in paintings include increases in transparency (Shimadzu & van den Berg, 2006) and adhesion failure between layers causing flaking and loss (Rogola et al., 2010).

Until recently, studies of zinc soap related degradation phenomena have been limited to the later stages of degradation, when zinc soap rich domains become detectable with visible or Fourier Transform infrared microscopy techniques. If we want to develop strategies to halt or slow zinc soap accumulation, it is necessary to focus attention on the initial stages in the nanometer

Author for correspondence: John Drennan, E-mail: j.drennan@uq.edu.au

Cite this article: Hermans J, Osmond G, van Loon A, Iedema P, Chapman R, Drennan J, Jack K, Rasch R, Morgan G, Zhang Z Monteiro M, Keune K (2018) Electron Microscopy Imaging of Zinc Soaps Nucleation in Oil Paint. *Microsc Microanal* **24**(3): 318–322. doi: 10.1017/S1431927618000387

region: the nucleation of zinc soap in the polymerized oil matrix and the subsequent transport of zinc and fatty acids that facilitates zinc soap growth.

Materials and Methods

As a model system, ZnO was mixed with linseed oil and water, allowed to react, and finally cured as a film over a few weeks at room temperature in air. A relatively low concentration of pigment was chosen in this system to enable easy distinction between ZnO particles or zinc soap phases and the surrounding polymer, as well as to promote rapid formation of zinc soaps through the presence of a large excess of fatty acids.

Paint reconstructions were prepared by stirring ZnO (0.5 g; Sigma Aldrich, St Louis, MO, USA) with cold-pressed untreated linseed oil (3.0 g; Kremer Pigmente, New York, NY, USA) and demineralized water (1 mL) in a sealed vial at room temperature for 3 days. After allowing the mixture to settle, it was left to dry in air at room temperature for up to 7 weeks.

Scanning electron microscopy was undertaken on samples of the paint reconstructions which were removed from glass slides and simply mounted on metallic stubs using conductive epoxy. No other mounting system was necessary in the 3-View system. The 3-View system is supplied by Gatan and consists of a microtome blade within the chamber of a scanning electron microscope. The scanning electron microscope in the case was a Zeiss Sigma 3-View (Cambridge, UK), low vacuum, with a field emission gun. The backscattered detector in the system is tuned and designed specifically for recording images at low accelerating voltages. The images were recorded after each 50 nm cut, in backscattered mode at an accelerating voltage of 1.2 keV.

Analytical transmission electron microscopy (TEM) was undertaken on microtomed cut sections transferred to a copper grid coated with a thin layer of carbon. The microscope was JEOL 2100 (JEOL Ltd., Tokyo, Japan), operating at 200 keV. For electron tomography, 300 nm thick sections were cut from the samples using Leica EM UC6 ultramicrotome (Leica Microsystems, Wetzlar, Germany). Dual-axis tilt-series data were collected on an FEI Tecnai F30 FEG-TEM (FEI Company, Hillsboro, OR, USA) operating at 300 kV, over a tilt range of +/−70° at 1.5° increments, using SerialEM software (The Boulder Lab for 3D Electron Microscopy, USA). Tilt-series were reconstructed with the R-weighted back projection algorithm using IMOD/Etomo software (The Boulder Lab for 3D Electron Microscopy, Boulder, CO, USA), and segmented using IMOD's automated isosurface rendering function.

Fourier transform infrared spectra (FTIR) were averaged over 16 scans and recorded at 4 cm^{-1} resolution using a Varian 660-IR FT-IR spectrometer (Palo Alto, CA, USA) combined with a Pike Technologies diamond GladiATR unit (Fitchburg, WI, USA).

Small angle X-ray scattering (SAXS) was performed using an Anton Paar SAXSess instrument (Anton Paar GmbH, Graz, Austria). The instrument is a compact Kratky design and uses a copper anode source (operating at 40 kV and 40 mA) and a Princeton CCD detector (Princeton Instruments, Hudson, NH, USA). Scattered data were collected at room temperature, and the data were reduced to remove background scattering and also desmeared.

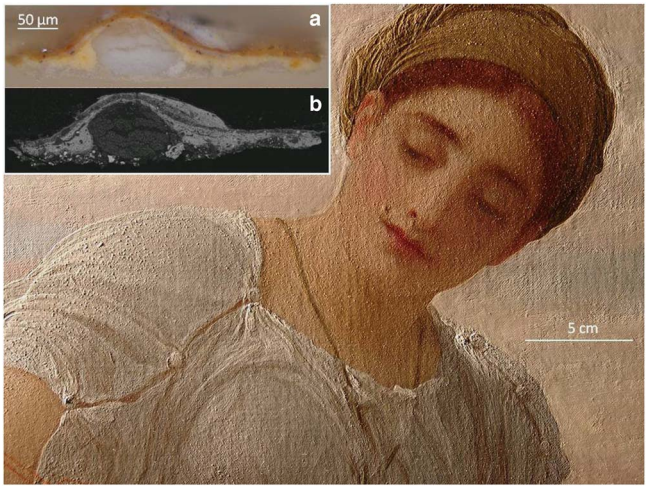

Figure 1. Frederic Leighton, *Winding the skein*, c. 1878. Art Gallery of New South Wales. Purchased 1974, photographed in raking light showing part of one of the figures affected by zinc soap aggregates which impart a pimpled texture to the paint. Inset: paint cross section taken from brown paint (**a**) optical and (**b**) backscatter electron image showing the distinct morphology of the zinc soap which has deformed overlying paint layers. Image reproduced with permission, Art Gallery of New South Wales.

Results

Figure 2 shows a backscatter electron micrograph recorded on a scanning electron microscope equipped with the GATAN 3-view system. This instrument allows *in situ* serial cutting of thin sections and uses a detector that it is extremely sensitive to back-scattered electron contrast even at very low accelerating voltages. The image presented in Figure 2 reveals several contrast features. Here the contrast is reversed from the usual convention, with atomically heavier features appearing as black. This is designed to enable comparison of scanning electron backscattered images with transmission images of the same features. There is an overall gray dense background, small (200 nm) black remnant ZnO particles and mid-gray flower-like regions scattered throughout the sample. The striations running vertically over the length of the images are the result of the soft surface of the sample buckling and stretching under the influence of the diamond cutting blade. The direction of cut is from the left to the right of the image.

Following observation and identification of these microstructural features in the scanning electron microscopy (SEM), microtome sections suitable for examination by analytical TEM were prepared. The SEM images were crucial for guiding subsequent investigation to support the interpretation of the intermediate gray structures as zinc soaps. Correlated microscopy and backscattered micrographs taken at lower magnification enabled location of key features for further examination at higher magnification. Figure 3a shows a TEM image of one of the intermediate gray features with a corresponding Zn energy dispersive X-ray map. It is clear that the flower-like features are strongly enriched in Zn compared to the

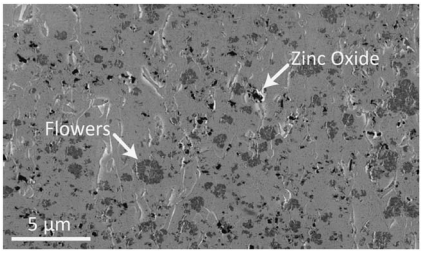

Figure 2. Backscattered scanning electron microscope image recorded at 1.2 keV. The sample surface was prepared by cutting with a microtome blade inside the chamber of the microscope. Light gray "flowers" are marked on the image, and these are zinc stearate precipitates. Small dark particles are remnant ZnO particles.

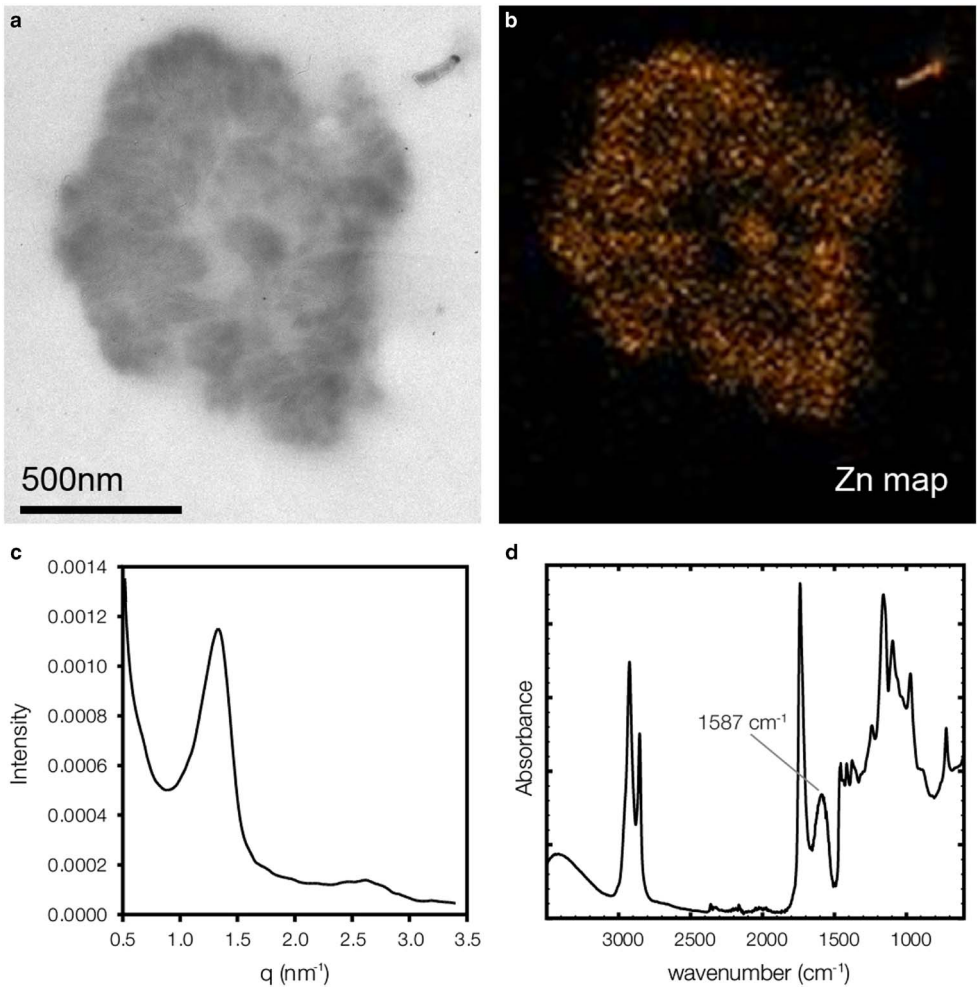

Figure 3. Characterization of the precipitates shown in Figure 2. (**a**) Transmission electron micrograph at a low resolution of the precipitates identified in Figure 2. (**b**) EDX Zn map from the same precipitate and (**c**) is a small angle x-ray scattering trace showing the interlayer spacing expected of zinc stearate. (**d**) Bulk Fourier Transform Infrared Spectrum of a sample of ZnO in linseed oil, which shows a zinc carboxylate band at 1587 cm^{-1}.

background. The presence of zinc soaps in the model system is further corroborated by the SAXS results in Figure 3c. The two peaks at 1.35 and 2.65 nm^{-1} are indicative of a lamellar metal soap structure. Moreover, the corresponding d-spacing obtained from the two observed peaks (with $d = 2\pi/q$) of ~46.5 Å is close to the reported value for pure zinc stearate of 42.8 Å (Hermans et al., 2015). The difference is most likely due to the significantly lesser degree of long-range ordering of the parallel plates in these samples compared with pure zinc stearate which leads to greater peak broadening and consequent uncertainty.

A bulk ATR-FTIR spectrum of this system (Fig. 3d) shows a broad carboxylate band centered at 1587 cm^{-1}. We have previously demonstrated that such a carboxylate band can be attributed to amorphous zinc soaps or *ionomer*-like zinc carboxylate (Hermans et al., 2015, 2016*a*). Though the SEM and TEM images suggest that the system contains a mixture of (semi-) crystalline zinc soaps and ionomer-like polymer medium, the IR spectrum only contains a broad zinc carboxylate band associated with amorphous zinc carboxylates. The lack of any crystalline metal soap features could mean that the zinc soap accumulations are still too disordered to exhibit sharp IR bands and are actually contributing to the broad-band in Figure 3d. This interpretation is supported by the work of MacDonald et al. (2016), who found very similar domains of (semi-) crystalline metal carboxylate in ethyl linoleate reacted with lead or zinc acetate. In that system, XRD of an isolated metal carboxylate accumulation showed some weak crystalline features, while an FTIR spectrum of the same sample exhibited only a broad amorphous metal carboxylate band. Alternatively, it could be the case that, despite the apparent abundance of zinc soaps in Figure 2, the zinc soaps only constitute a very small fraction of the total population of zinc carboxylate species, meaning that the FTIR spectrum is still dominated by ionomeric zinc carboxylates.

We believe the evidence that has been presented so far suggests that these flowers are the initial precipitation of zinc soap phases. The high number of the smaller zinc soap flowers and their homogeneous distribution throughout the film indicates that nucleation of zinc soap phases is not a rare phenomenon under these conditions. Even on this relatively short timescale and in this region of the sample, there has been extensive degradation of the pigment, and very little intact ZnO remains. Interestingly, there seems to be no correlation between the location of remaining ZnO particles and the zinc soaps, so crystallization obviously does not happen near the surface of pigment particles. A more detailed three-dimensional reconstruction of this data is shown in Figure 1 of the Supplementary Material.

Figure 4 provides the detailed image of the precipitation processes taking place. Recorded using a highly sensitive electron detection camera and low dose technology, these high-resolution

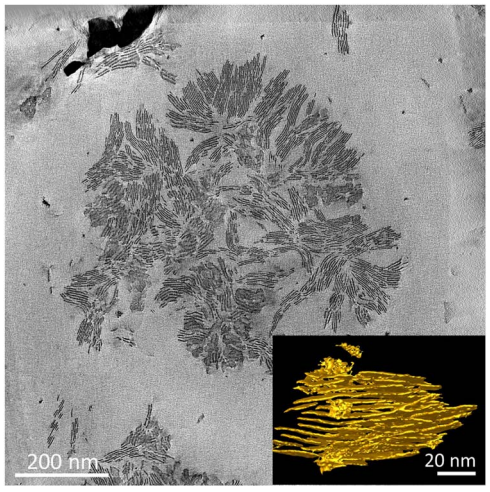

Figure 4. Transmission electron microscope bright field image showing the start of the precipitation of zinc soap. Inset is a frame from the three-dimensional reconstruction (full movie shown in the extended data) showing the plate-like structure of the precipitate. The distance between plates is ~4.2 nm. The electron-dense region in the top left of the image is either a remnant zinc oxide particle or contamination introduced during processing.

images reveal the microstructure of one flower-like accumulation. In this instrument, we were able to perform a tilt series in order to build a tomogram. The full interactive tomogram is presented in the Supplementary Material. The micrograph reveals that the flower-like structures consist of parallel plates that appear to fan out from a central region. The black lines represent the carboxylate coordinated zinc plates in the zinc soap structure (Lacouture et al., 2000). Because of the random orientation of the individual crystalline domains relative to the electron beam, some regions seem to contain more closely spaced zinc plates while some appear as textured smudges. The spacing between the layers was calculated by taking the average of many measurements of the interlayer distance within one domain oriented roughly perpendicular to the plane of the image. The interlayer spacing was found to be 45 ± 4 Å, which is similar to the spacings reported for zinc palmitate (38.5 Å) and zinc stearate (42.8 Å) (Hermans et al., 2014), The crystalline domains consist of layers of these plates and are roughly 50–100 nm in size. The relatively wide range of measured spacings as well as the abundance of rough edges, breaks, and curvature in the zinc-containing planes all suggest that there is still significant disorder in the packing of alkyl chains and/or metal ion coordination. Moreover, in many cases, the domains are separated by regions of linseed oil polymer. These observations suggest that zinc soap crystallization is in its early stages. Once zinc soap precipitation has begun, the natural tendency to reduce the surface area of the precipitate will encourage continuing diffusion of zinc atoms and fatty acids towards the growing aggregate while the free energy of the system is further reduced by improving fatty acid chain packing. In a process related to Ostwald ripening, it can be envisaged that growth of larger precipitates will occur at the expense of smaller precipitates, leading to large masses similar to those presented in Figure 1.

Conclusion

The data presented provides the first evidence of the earliest stages of metal soap formation in oil paintings. The low concentration of ZnO in the model has allowed detailed visualization of this process. In a real paint, the higher pigment density and more complex composition may inhibit distinctive precipitation. For oil paintings containing zinc white, the question remains as to whether it is possible to prevent disfiguring soap formation. Our current observations and previous work suggest that once ZnO has been mixed with an oil medium, eventual metal soap formation is inevitable. Particle properties, fatty acid composition, and environmental variables will influence the rate of formation, but reversing the process of zinc soap phase separation seems an immense challenge (Hermans et al., 2016*b*). For the present, we will continue to study factors that govern mobility of metal ions and fatty acids in the polymerized oil system, while optimizing storage conditions and conservation treatments to minimize growth of aggregates in susceptible paintings.

Through attempts to address a challenge in art conservation, the electron microscopy techniques explored here have application across a wide range of soft materials characterization challenges. The quality of electron detectors combined with specially optimized sample preparative methods lessons opens up correlated characterization regimes for a wide range of (heterogeneous) materials. Microstructural analysis becomes possible for materials that were too difficult to image in the past.

Supplementary material. To view supplementary material for this article, please visit https://doi.org/10.1017/S1431927618000387

Acknowledgments. A major part of the work was undertaken during a sabbatical visit by Professor Drennan that was hosted by the Van't Hoff Institute for Molecular Sciences, University of Amsterdam.

The authors also acknowledge the facilities, and the scientific and technical assistance, of the Australian Microscopy & Microanalysis Research Facility at the Centre for Microscopy and Microanalysis, The University of Queensland.

References

Centeno SA and Mahon D (2009) The chemistry of aging in oil paintings: Metal soaps and visual changes. *MMAB* **67**(1), 12–19.

Chen-Wiegart YK, Catalano J, Williams GJ, Murphy A, Yao Y, Zumbulyadis N, Centeno SA, Dybowski C and Thieme J (2017) Elemental and molecular segregation in oil paintings due to lead soap degradation. *Sci Rep* **7**(1), 11656.

Harley RD (1970) *Artists' Pigments c.1600-1835*. London: Butterworth and IIC.

Helwig K, Poulin J, Corbeil M-C, Moffat E and Duguay D (2014) Conservation issues in several 20th –century Canadian oil paintings: the role of zinc carboxylate reaction products. In: *Issues in Contemporary Oil Paint*, van den Berg KJ, Burnstock A, Keijzer M, Krueger J, Learner T, de Tagle A and Heydenreich G (Eds.), pp. 167–184. Cham, Switzerland: Springer International Publishing.

Hermans JJ, Keune K, Van Loon A, Corkery RW and Iedema PD (2014) The molecular structure of three types of long chain zinc(II) alkanoates for the study of oil paint degradation. *Polyhedron* **81**, 335–340.

Hermans JJ, Keune K, Van Loon A, Corkery RW and Iedema PD (2016*a*) Ionomer-like structure in mature oil paint binding media. *RSC Adv* **6**, 93363–93369.

Hermans JJ, Keune K, Van Loon A and Iedema PD (2016*b*) The crystallisation of metal soaps and fatty acids in oil paint model systems. *Phys Chem Chem Phys* **18**, 10896.

Hermans JJ, Keune K, Van Loon A and Iedema PD (2015) An infrared spectroscopic study of the nature of zinc carboxylates in oil paintings. *J Anal At Spectrom* **30**, 1600–1608.

Higgett C, Spring M and Saunders D (2003) Pigment –medium interactions in oil-paint films containing red lead or lead – tin yellow. *Natl Gallery Tech Bull* **24**, 75–95.

Kaszowska Z, Malek K, Panczyk M and Mikolajska A (2013) A joint application of ATR-FTIR and SEM imaging with High spatial resolution: Identification and distribution of painting materials and their degradation products in paint cross sections. *Vib Spectrosc* **65**(2013), 1–11.

Keune K and Boeve-Jones G (2014) Its surreal: zinc-oxide degradation and misperceptions in Salvador Dali's *Couple with clouds in their heads, 1936*. In: *Issues in Contemporary Oil Paints*, van den Berg KJ, Burnstock A, Keijzer M, Krueger J, Learner T, de Tagle A and Heydenreich G (Eds.), pp. 283–294. Cham, Switzerland: Springer International Publishing.

Keune K and Boon JJ (2007) Analytical imaging studies of cross-sections of paintings affected by lead soap aggregate formation. *Studies in Conservation* **56**(3), 161.

Kuhn H (1986) Zinc white. In: *Artists' Pigments*, vol 1. Feller RL (Ed.), pp. 169–186. Cambridge: Cambridge University Press.

Lacouture F, **Peultier J**, **Francois M and Steinmetz J** (2000) Anhydrous polymeric zinc(II) octanate. *Acta Cryst C* **56**(5), 556–557.

MacDonald MG, **Palmer MR**, **Suchomel MRBerrie BH** (2016) Reaction of Pb(II) and Zn(II) with ethyl linoleate to form structured hybrid inorganic–organic complexes: a model for degradation in historic paint films. *ACS Omega* **1**(3), 344–350.

Noble P, **Boon JJ and Wadum J** (2002) Dissolution aggregation and protrusion: lead soap formation in 17th century grounds and paint layers. *Art Matters* **1**, 46–61.

Osmond G, **Ives S**, **Dredge P**, **Drennan J and Puskar L** (2013) From Porcelain to Pimples a Study of Synchrotron-sourced Infrared Spectroscopy for Understanding the Localised Aggregation of Zinc Soaps in a Painting by Sir Fredrick Leighton. Poster presented at the 7th International Workshop on Infrared Microscopy and Spectroscopy with Accelerator Based Sources, Lorne, 10–14 November 2013.

Osmond G, **Keune K and Boon JJ** (2005) A study of zinc soap aggregates in late nineteenth century paintings by R. G. Rivers at the Queensland Art Gallery. *AICCM Bull* **29**, 37–46.

Osmond G (2012) Zinc white: a review of zinc oxide pigment properties and implications for stability in oil-based paintings. *AICCM Bull* **33**, 20–29.

Plater M, **De Silva B**, **Gelbrich T**, **Hursthouse MB**, **Higget CL and Saunders DR** (2003) The characterisation of lead fatty acid soaps in "protrusions" in aged traditional oil paint. *Polyhedron* 22(24), 3171–3179.

Shimadzu Y and Van Den Berg KJ (2006) On metal soap related colour and transparency changes in a 19th century painting by Millais. In: *Reporting Highlights of the de Mayerne Programme. Netherlands Organisation for Scientific Research, The Hague*, Boon JJ and Ferreira ESB (Eds.), pp. 43–52. Amsterdam: University of Amsterdam.

Townsend J, **Jones R and Stoner K** (2007) Lead soap aggregates in sixteenth and seventeenth century British Paintings. in: *AIC Paintings Speciality Group Post Prints, Providence, Rhode Island, 16-19 June 2006*, Mar Parkin H (Ed.), pp. 24–32. New York: AIC.

Van der Weerd J, **Gelddof M**, **Vander Loff LS**, **Heeren R and Boon JJ** (2003) Zinc soap aggregate formation in Falling Leaves (Les Alyscamps) by Vincent van Gogh. *Zeetschrift fur Knusttechnologie und Konservierung* **17**(2), 407–416.